JCI insight

Clinical and pathological investigation of severe COVID-19 patients

Shaohua Li, … , Junsheng Ji, Jingmin Zhao

JCI Insight. 2020. https://doi.org/10.1172/jci.insight.138070.

Research In-Press Preview COVID-19 Infectious disease Pulmonology

BACKGROUND. Severe acute respiratory coronavirus 2 (SARS-CoV-2) caused coronavirus disease 2019 (COVID-19) has become a pandemic. This study addressed the clinical and immunopathological characteristics of severe COVID-19.

METHODS. Sixty-nine COVID-19 patients were classified into as severe and non-severe groups to analyze their clinical and laboratory characteristics. A panel of blood cytokines was quantified over time. Biopsy specimens from two deceased cases were obtained for immunopathological, ultrastructural, and in situ hybridization examinations.

RESULTS. Circulating cytokines, including IL8, IL6, TNFα, IP10, MCP1, and RANTES, were significantly elevated in severe COVID-19 patients. Dynamic IL6 and IL8 were associated with disease progression. SARS-CoV-2 was demonstrated to infect type II, type I pneumocytes and endothelial cells, leading to severe lung damage through cell pyroptosis and apoptosis. In severe cases, lymphopenia, neutrophilia, depletion of $CD4^+$ and $CD8^+$ T lymphocytes, and massive macrophage and neutrophil infiltrates were observed in both blood and lung tissues.

CONCLUSIONS. A panel of circulating cytokines could be used to predict disease deterioration and inform clinical interventions. Severe pulmonary damage was predominantly attributed to both SARS-CoV-2 caused cytopathy and immunopathologic damage. Strategies that encourage pulmonary recruitment and overactivation of inflammatory cells by suppressing cytokine storm might improve the outcomes of severe COVID-19 patients.

Find the latest version:

https://jci.me/138070/pdf

Clinical and pathological investigation of severe COVID-19 patients

Shaohua Li1#, Lina Jiang1#, Xi Li1#, Fang Lin2#, Yijin Wang1#, Boan Li3#, Tianjun Jiang4#, Weimin An5, Shuhong Liu1, Hongyang Liu1, Pengfei Xu1, Lihua Zhao1, Lixin Zhang1, Jinsong Mu2, Hongwei Wang6, Jiarui Kang6, Yan Li1, Lei Huang4, Caizhong Zhu4, Shousong Zhao7, Jiangyang Lu6, Junsheng Ji4, Jingmin Zhao1*

1 Department of Pathology and Hepatology, The Fifth Medical Center of PLA General Hospital, Beijing, China

2 Department of Intensive Care Unit, The Fifth Medical Center of PLA General Hospital, Beijing, China

3. Department of Clinical Laboratory, The Fifth Medical Center of PLA General Hospital, Beijing, China

4. Department of Infectious Diseases, The Fifth Medical Center of PLA General Hospital, Beijing, China

5. Department of Radiology, The Fifth Medical Center of PLA General Hospital, Beijing, China

6. Department of Pathology, The Fourth Medical Center of PLA General Hospital, Beijing, China

7. Department of Infectious Diseases, First Affilitated Hospital of Bengbu Medical College, Bengbu, China

Address reprint requests to Dr. J. Zhao at Department of Pathology and Hepatology, The Fifth Medical Center of PLA General Hospital, No. 100 Xi Si Huan Middle Road, Beijing 100039, China, or at 0086-10-66933262, jmzhao302@163.com.

Drs. SLi, LJ, XL, FL, YW, BL and TJ contributed equally to this article.

Declaration of Interests: The authors have declared that no conflict of interest exists.

Declaration of submission: We declare that the paper has not been submitted to another journal, and has not been published in whole or in part elsewhere previously.

FUNDING

There is no funding.

ABSTRACT

BACKGROUND

Severe acute respiratory coronavirus 2 (SARS-CoV-2) caused coronavirus disease 2019 (COVID-19) has become a pandemic. This study addressed the clinical and immunopathological characteristics of severe COVID-19.

METHODS

Sixty-nine COVID-19 patients were classified into as severe and non-severe groups to analyze their clinical and laboratory characteristics. A panel of blood cytokines was quantified over time. Biopsy specimens from two deceased cases were obtained for immunopathological, ultrastructural and in situ hybridization examinations.

RESULTS

Circulating cytokines, including IL8, IL6, TNFα, IP10, MCP1 and RANTES, were significantly elevated in severe COVID-19 patients. Dynamic IL6 and IL8 were associated with disease progression. SARS-CoV-2 was demonstrated to infect type II, type I pneumocytes and endothelial cells, leading to severe lung damage through cell pyroptosis and apoptosis. In severe cases, lymphopenia, neutrophilia, depletion of CD4+ and CD8+ T lymphocytes, and massive macrophage and neutrophil infiltrates were observed in both blood and lung tissues.

CONCLUSIONS

A panel of circulating cytokines could be used to predict disease deterioration and inform clinical interventions. Severe pulmonary damage was predominantly attributed to both SARS-CoV-2 caused cytopathy and immunopathologic damage. Strategies that encourage pulmonary recruitment and overactivation of inflammatory cells by suppressing cytokine storm might improve the outcomes of severe COVID-19 patients.

KEY WORDS

COVID-19; SARS-CoV-2; severe disease; cytokines; pathology

INTRODUCTION

Severe acute respiratory coronavirus 2 (SARS-CoV-2) causes coronavirus disease 2019 (COVID-19), which is an emerging respiratory infectious disease that has become an overwhelming health threat globally. SARS-CoV-2 has affected more than 2 million individuals, and caused nearly 120 thousand deaths, resulting in an average mortality of 6.33% worldwide as of Apr 14th, 2020, compared with the mortality rate of less than 1% of influenza. The spectrum of SARS-CoV-2 infection ranges from asymptomatic and mild symptoms, to pneumonia and life-threatening complications, including acute respiratory distress syndrome (ARDS), septic shock, multi-organ failure, and ultimately death (1, 2). Notably, about 11% of mild patients show a sharp deterioration that result in severe manifestations, including respiratory failure, multi-organ failure or even death (3). The fatality rate of critical COVID-19 patients was shown to be approximately 61.5% (4). Therefore early warning and management of severe COVID-19 individuals still face a big challenge.

To date, host risk factors have been identified to be associated with critical illness and mortality in COVID-19 patients, but rarely have early signs of the risk of disease progression been reported. Extensive studies have revealed that severe COVID-19 cases are more likely to present lymphopenia, hypoalbuminemia, and higher lactate dehydrogenase, C-reactive protein (CRP), ferritin and D-dimer (2, 3, 5). Both severe acute respiratory syndrome (SARS) and COVID-19 are characterized by an overexuberant inflammatory response that is associated with disease severity. Evidence has shown that CD4+ and CD8+ T lymphocytes were significantly decreased with down-regulated IFNγ expression, while the levels of pro- and anti-inflammatory cytokines, including IL2R, IL6, IL10 and TNFα were remarkably increased (6, 7). However, whether SARS-CoV-2 *per ser* or viral infection induced dysregulated immune response contributing to severe lung damage warrants further investigation. In addition, the dynamics of cytokines, pulmonary inflammatory infiltration and links between abnormal immune response and immunopathology in the lung in COVID-19 remain to be elucidated, which is vital for clinical management of the disease.

The objective of this study is to fulfill the gap between clinical and pathological analysis to provide insights into clinical management of severe patients, and to explore the immunopathological features of COVID-19. We hereby assessed the predictors of deterioration by performing detailed comparisons of clinical, radiologic, laboratory and dynamic cytokine data between severe and non-severe patients. The signs of deterioration were further assessed by examination of the immuno- and ultrastructural pathology of postmortem biopsy specimens from two severe patients.

RESULTS

Epidemiology and clinical presentation

Thirty-six of 69 patients had a definite history of exposure in Hubei. Among the 69 patients, 19 were diagnosed as severe condition on admission, and 7 patients progressed to severe condition during hospitalization. Three patients were transferred to intensive care units (ICU), and 2 patients died of ARDS (8) and septic shock caused by *Klebsiella Pneumoniae*, respectively. Forty-three patients were diagnosed as non-severe condition.

Fever, cough, headache, diarrhea and sore throat were common at the onset of illness. Most of the patients had more than one sign or symptom. Compared with non-severe patients, severe patients were significantly older (58 (45-75) vs. 39 (29-53); p<0.001), and more likely to report myalgia or fatigue (14 (53.9) vs. 12 (27.9); p=0.031) and dyspnea (7 (26.9) vs. 1 (2.3); p=0.004) (Table 1). Severe patients had a higher prevalence of chronic liver disease compared to non-severe patients (3 (11.5) vs. 0 (-), p=0.05). The gender distribution, endemic history, and prevalence of underlying comorbidities such as diabetes, hypertension, cardiovascular disease and chronic respiratory system disease did not differ between severe and non-severe patients (p>0.05) (Table 1). Typical chest radiogram findings include bilateral pulmonary parenchyma ground glass, consolidative pulmonary opacity, and the number of lobes affected by ground glass or combined opacity (Figure 1 A-H). Disease severity was associated with higher radiology scores (p<0.001).

Most patients received antiviral therapy with interferon α2b by inhalation and Lopinavir/Ritonavir orally. Systemic corticosteroid therapy (96.2% vs. 11.6%, p<0.001) and intravenous immunoglobulin therapy (80.8% vs. 16.3%, p<0.001) were administered more often in severe patients than in non-severe patients (Table 1). Intravenous antibiotics (88.5% vs. 7%, p<0.001) and antifungal medication (46.2% vs. N.A., p<0.001) were administered more frequently in severe patients. In regard to respiratory support, oxygen therapy, especially with a high flow nasal cannula, was applied more often to severe patients than to non-severe patients (p<0.001). More severe patients received ventilation support (5 with noninvasive ventilation and 2 with invasive ventilation, p=0.006). One patient received extracorporeal membrane oxygenation (ECMO), and 4 patients received continuous renal replacement therapy (CRRT). At follow-up, 60 of 69 patients completely recovered, 7 patients were still in ward, and 2 patients died. The length of stay of severe patients was longer than that of non-severe patients (23 days vs. 14 days, p<0.001) (Table 1).

Laboratory tests and cytokines in severe and non-severe patients

Of the 26 severe patients, 88% had a PaO2/FIO2 value less than 300; 96% of severe patients had a SpO2 value less than 93%; and 35% of severe patients had a respiratory rate (RR) greater than 30 breaths/min. A SpO2 value ≤93% at rest was the most useful parameter for defining severity. The pressure of oxygen (68 vs. 85, p<0.001) and oxygenation index (262 vs. 393, p<0.001) were much lower in severe group than that in non-severe group. The alveolar-arterial oxygen partial pressure difference (A-aDO2, 52 vs. 23, p<0.001) was higher than that in non-severe patients (Table 2).

There were significant differences in a panel of laboratory tests between severe and non-severe patients, including cell counts of lymphocytes, neutrophils and eosinophils (p<0.05, respectively). We observed a significant decrease in CD4+ and CD8+ T

cells in severe patients ($p<0.05$, respectively). High levels of blood fibrinogen and D-dimer were present in severe patients ($p<0.05$, respectively). In regard to biochemical parameters, albumin (34 vs. 42, $p<0.001$), γ-glutamyl transferase (GGT, 50 vs. 22, $p<0.001$) and lactate dehydrogenase (LDH, 247 vs. 197, $p<0.001$), in severe patients were within normal ranges but showed abnormal tendencies, and were significantly different from those in non-severe patients (Table 3). There were significant elevations in blood glucose (8.1 vs. 5.0, $p<0.001$), Apo-A1 (0.80 vs. 1.08, $p<0.001$), pro-brain natriuretic peptide (pro-BNP, 217.7 vs. 22.9, $p<0.001$), erythrocyte sedimentation rate (ESR, 54 vs. 13, $p<0.05$), ferritin (FER, 645 vs. 254, $p<0.05$) and C-reactive protein (CRP, 22.2 vs. 4.2, $p<0.05$) in severe patients (Table 2). Notably, the levels of IL8 (13.1 vs. 7.8, $p<0.001$), TNFα (7.4 vs. 5.0, $p<0.001$), IL6 (24.6 vs. 8.4, $p<0.001$), MCP1 (264 vs. 134, $p=0.001$), IP10 (863 vs. 372, $p<0.001$) and RANTES (2272 vs. 2074, $p<0.001$) were elevated in severe group than those in non-severe group (Table 2).

The kinetics of blood neutrophils, lymphocytes, monocytes, IL6, IL8, D-dimer, CRP and glucose based on consecutive samples obtained at 2-day intervals were determined within 11 days from admission day. In severe group, neutrophilia rose to peak while lymphopenia reached the lowest point on 7th day (Figure 2A, 2B). Fluctuation of monocyte counts was observed in both severe group and non-severe group (Figure 2C). Glucose sustained at a high level, CPR sustained a decrease, and D-dimer continued to increase during the disease course of COVID-19 in severe patients. (Figure 2D-F). Figure 2G-H revealed that the levels of IL6 and IL8 on admission were remarkably higher in severe group compared with non-severe group. Subsequently, the level of IL6 in severe group showed a rapid increase with a peak level on day 5 of hospitalization, on average. While serum IL8 had sustained high level until hospital day 5. The dynamics of IL6 and IL8 concentrations were highly consistent with disease deterioration.

Histopathological findings

In reference to pathology staging of SARS (5), in this study, early phase was defined as a disease course of 7 to 14 days, with features of acute exudative diffuse alveolar damage (DAD). Late phase was defined as a disease course lasting more than 14 days, or even longer, with features of organizing and fibrotic DAD. Histological examination of lung tissues from two cases representative of acute phase (Figure 3) and late phase (Figure 4) of the disease showed varied pathological features. Case 1 (disease course of 14 days) showed DAD, acute exudative edema, hyaline membrane formation, and desquamation of pneumocytes, which was consistent with the features of early stage (Figure 3A). In case 2 (disease course of 28 days), H&E and Masson's trichrome stains showed features of interstitial and alveolar fibrosis and pneumocyte hyperplasia with focal exudative edema and hyaline membrane in alveolar spaces, indicating late stage pathology of the disease (Figure 4A-B). In these two cases, multinucleated pneumocytes were identified, indicating viral cytopathic-like changes. Viral inclusions were not detected.

Ultrastructural findings

Ultrastructural study of lung tissues from two cases revealed typical viral particles in cytoplasm of pneumocytes, especially in type II pneumocytes, with or without membrane-bound vesicles. The virus particles were spherical and enveloped, spike-like projections on the surface, most ranged from 60 to 120 nm in diameter, indicating characteristic coronavirus particles (Figure 3B, 4C). Pneumocytes appeared markedly swollen mitochondria and dilated endoplasmic reticulum. Type II pneumocytes presented hyperplasia with lager nuclei and nucleus, and depleted laminar bodies. Endothelial cells of small blood vessels were swollen

and vacuolated.

Immunohistochemical findings

Immunohistochemical staining for surfactant protein B (SPB) and CK7 showed damaged type II pneumocytes with mild to moderate hyperplasia (Figure 3C-D, 4D-E). The number of CD68+ macrophages with cytomegalic feature were significantly increased in alveolar spaces in lung tissues from both deceased cases (Figure 3E, 4F). In case 2, some CD68+ cells were foamy or vacuolated (Figure 4F). Numerous neutrophils were observed in the interstitial infiltrates, predominantly in bronchopneumonia in case 2 (Figure 3F, 4G). CD4+ and CD8+ T cells were scattered in lung tissues (Figure 3G-H, 4H-I). Many gasdermin D+ pneumocytes in case 1 and moderate number of gasdermin D+ pneumocytes in case 2 appeared, which indicated that the main pattern of cell death involved pyroptosis in lung tissues of COVID-19 patients (Figure 3I, 4J). TUNEL staining indicated an increase of apoptotic cells (40-50 positive cells in case 1 and 15-20 positive cells in case 2, per 200X magnification), reflecting an alternative manner of cell death (Figure 3J-K, 4K-L).

RNAscope in situ hybridization findings

Positive signals of RNAscope in situ hybridization were spotted brown particles within SARS-CoV-2 infected cells. Negative controls for in situ hybridization performed with an irrelevant probe showed no positive signal in lung tissues. In situ hybridization results indicated that SARS-CoV-2 RNA was distributed in cytoplasm of many pneumocytes, some macrophages and endothelial cells (Figure 3L, 4M), but no positive signal was detected in infiltrating lymphocytes in lung tissues from both cases.

DISCUSSION

This study addressed the features of severe COVID-19 by comprehensive analysis of clinical, laboratory, radiologic, and pathology. The results showed an overexuberant response of a panel of pro-inflammatory cytokines including IL8, IL6, TNFα, IP10, MCP1 and RANTES in severe patients, and dynamics of serum IL6 and IL8 were closely associated with disease progression. As a lung tropic virus, SARS-CoV-2 infected type II, type I alveolar epithelial cells, as well as endothelial cells in small blood vessels were demonstrated by both TEM and in situ hybridization, leading to lung damage with cell death patterns of pyroptosis and apoptosis. The underlying mechanisms of cytokine storm and lung damage involved the exhaustion of CD4+ and CD8+ T cells followed by massive infiltration of macrophages and neutrophils into lung tissues, causing the dysregulation of pro-inflammatory cytokines and chemokines.

Clinically, three criteria, the PaO2/FIO2 ratio, SpO2 and RR are often used to define severe COVID-19 patients. In our cohort, since 96% of severe patients had a SpO2 value ≤ 93% at rest, it seems that SpO2 is the most useful indicator for defining disease severity. Elder and severe symptoms of myalgia, fatigue and dyspnea were the most common features of severe patients, as described in other previous reports (2, 3, 7). Lymphopenia is a common feature with drastically reduced numbers of CD4+ T cells, CD8+ T cells and B cells (5, 8, 9).Reduced percentages of monocytes and eosinophils are also common. An increase in the neutrophil-to-lymphocyte ratio usually indicates increased disease severity and a poor clinical outcome. In our cohort, dynamic tests in severe patients indicated that lymphopenia with remarkable decrease of CD4+ and CD8+ T lymphocytes, neutrophilia,

and a sustained increase in neutrophil-to-lymphocyte ratio that reached a peak on the 7th day on admission, suggesting that physicians should monitor these dynamic characteristics in severe patients. The dramatic reduction in lymphocytes in severe patients might be caused by both overexuberant immune responses and SARS-CoV-2 infection of T lymphocytes (10). Neutrophilia in COVID-19 severity might be ascribed to abnormal elevated IL8 and granulocyte-macrophage colony stimulating factor (5). In our study, the substantial neutrophil infiltrate in lung tissues from the two deceased cases was assumed to indicate the possible role of neutrophilia in disease severity. In addition, some variables were identified to be associated with COVID-19 severity. An increase level of pro-BNP, as a predictor of heart dysfunction, was associated with disease deterioration. Additionally, increased levels of ferritin and glucose, while decreased level of albumin and Apo-A1 were found to correlate with COVID-19 severity, implying that severe patients were prone to metabolic disorders due to impaired liver function. However, we still lack conclusive evidence to support metabolic dysregulation by SARS-CoV-2 *per se*.

Previous studies have shown that increased levels of proinflammatory cytokines in blood (e.g., IL1B, IL6, IL12, IL17, IFNγ, IP10, MCP1, TNFα and IL15) were associated with pulmonary inflammation and extensive lung damage in SARS and MERS patients (11-13). Recent evidence suggested that most patients with severe COVID-19 exhibited substantially elevated serum levels of several cytokines, which can even manifest as cytokine storm (14). Consistently, our results showed that severe COVID-19 patients had an overexuberant response of a panel of pro-inflammatory cytokines and chemokines, including IL6, IL8, TNFα, IP10, MCP1 and RANTES than non-severe patients. These inflammatory factors are mainly derived from macrophages and neutrophils, which could be predictors of hypercytokinemia and systemic inflammatory response syndrome. Both IL6 and IL8 have been identified to recruit monocytes to drive inflammation by producing a set of chemokines in mice model of SARS(15). In this study, we found the dynamics of serum IL6 reflected a rapid increase with a peak level on day 5 of hospitalization, on average, while serum IL8 had maintained high level until day 5 of hospitalization in severe patients. The dynamic trends were highly consistent with disease deterioration. Indeed, in this cohort, systemic corticosteroids were administered to most severe patients, which might contribute to the interference of elevated IL6 and IL8 levels in severe patients. Based on the pathological findings of the massive recruitment of monocytes/macrophages and neutrophils to lung tissues, we speculated that the infiltrating inflammatory cells triggered or exacerbated inflammation and exudation, even ARDS in targeted lung, resulting in a vicious circle of cytokine release that led to cytokine storm.

In the absence of a proven effective therapy for severe COVID-19 patients, currently management consists of supportive care, usually including invasive and noninvasive oxygen support and antibiotic administration. Many patients have received off-label or compassionate-use therapies, including antivirals, anti-inflammatory compounds, and convalescent plasma (14, 16, 17). In our cohort from the early to middle period of the SARS-CoV-2 infection outbreak, the treatment strategies were empirically determined according our experiences with the SARS outbreak in 2003. However, the management of COVID-19 has rapidly evolved in the SARS-CoV-2 infection pandemic. In our cohort, 80.8% of severe patients received empirical antiviral therapy, including Ritonavir/Lopinavir and interferon α2b, 96.2% of severe patients received systematic corticosteroid therapy and 80.8% of cases administered intravenous immunoglobulin. In our cohort, the mortality was 7.7% for severe COVID-19 cases, which is lower than that reported by other centers (5, 18), however, the decrease in mortality could not be ascribed to treatments alone, and other factors such as the relatively young age [58(45-75)] of patients in our cohort could not be excluded. Hopefully, other

promising antiviral candidates, including hydroxychlorquine, Remdesivir and Favipiravir are undergoing clinical trials, and might provide potential antiviral options (19, 20). A recent study of on compassionate treatment with Remdesivir for severe COVID-19 patients reported an improved outcome in oxygen-support status and a decreased mortality of 13% compared to the reported 17%-78% mortality in severe cases (17). Another clinical trial result revealed that Favipiravir was independently associated with faster viral clearance of H1N1 flu, SARS-CoV and Ebola virus infections, encouraging the use of ongoing clinical trials for anti-SARS-CoV-2 infection (ChiCTR2000029600). For severe COVID-19 cases, supplemental oxygen therapy immediately to those with SARI and respiratory distress, hypoxaemia or shock should be emphasized. The two deaths in this study were due to pathological DAD with ARDS and septic shock caused by *Klebsiella Pneumoniae*, respectively. Thus prevention of ARDS and sepsis complications in severe COVID-19 patients is urgent. To suppress inflammatory cytokine storm or ARDS, corticosteroids are not regularly recommended for COVID-19 related lung injury or shock according to WHO guidance. Clark et al. recently reported that no good reason exists to expect COVID-19 patients to benefit from corticosteroids (21). The development of targeted therapeutics against cytokine storm is still a clinical issue. In our study, a panel of cytokines, IL6, IL8, IP10, TNFα, MCP1 and RANTES was profoundly elevated in severe patients during disease deterioration. Therefore, cytokine neutralization therapy is likely to be an alternative option. Recently, the preliminary data of a clinical trial of Tocilizumab (ChiCTR2000029765), a monoclonal antibody targeting IL6 receptor, showed improved outcomes in 21 severe COVID-19 patients. Other ongoing clinical trials of monoclonal antibodies targeting IL17 and TNFα, such as Secukinumab/Bimekizumab and Infliximab/Adalimumab (22) and so forth will hopefully provide evidence of efficacy against SARS-CoV-2. Additionally, convalescent plasma therapy also potentially benefits for severe patients with persistent viraemia (16).

SARS-CoV-2, a large, positive, single-stranded RNA coronavirus, is pneumophila, targeting the epithelial cells of the respiratory tract, resulting in pulmonary DAD. In this study, we demonstrated type II, type I pneumocytes and endothelial cells with conspicuous cytopathy in lung tissues were infected with SARS-CoV-2 by both TEM and in situ hybridization. Reactive hyperplasia of type II pneumocytes in DAD alveolar spaces in turn might facilitate virus infection and spreading due to high expression of angiotensin I converting enzyme 2. SARS-CoV-2 infection in endothelial cells in small vessels might contribute to vasculitis, even thrombosis, which was assumed to be related to increased blood D-dimer and fibrinogen levels in disease exacerbation. Thus severe pulmonary injury in SARS-CoV-2 patients was considered to result from both direct viral infection and immunopathological injury. Active cell death, in its many forms, is a fundamental disease process, especially for acute viral infection (23-25). The pathological findings of our study demonstrated that both pyroptosis and apoptosis contributed to lung damage, with pyroptosis as predominant cell death pattern. Pyroptosis is defined as gasdermin-mediated programmed necrosis in response to certain pathogen insults and is critical for immunity (26). A recent study revealed that caspases cleaved gasdermin D can switch between triggering caspase-3-mediated apoptosis and necrosis induced by TNF (27). In our severe cases, levels of TNFα and other factors were dramatically upregulated in blood, as well as severe inflammatory infiltrates in lung tissues, which could provide possible explanations of pyroptosis as the main pattern as to pulmonary damage.

COVID-19 is an emerging infectious disease and its immunopathology is highly complex. The possible mechanisms include the dysregulation of cytokines, deficiencies in the innate immune response, direct infection of immune cells and viral cytopathic effect, among which immunopathological damage to target organs is crucial for the exacerbation of COVID-19. In our study,

depletion of CD4+ and CD8+ T cells in both blood and lung tissues from severe COVID-19 patients suggested the exhaustion of T cells following abnormal activation. A study showed that feline enteric coronavirus infection induced the production of IL10 and skewed the immune response away from a protective Th1-cell response towards a non-protective Th2-cell response, thereby diminishing the ability of immune cells to clear the virus (28). Similarly, in severe COVID-19 cases, impaired cellular immunity is likely not only to delay viral clearance, but also to attack lung tissues directly or indirectly. Even more troubling, viral infection might interfere with the normal feedback mechanisms that control inflammation, and proinflammatory chemokines or other cytokines might be produced in large amounts or for an excessive period. Elevated levels of IL8, IL6, TNFα and IP10 might mediate extensive pulmonary pathology, leading to massive infiltration of neutrophils and macrophages, severe DAD, even ARDS, which is indicative of immune-mediated damage in severe patients. Collectively, impaired adaptive immune responses and uncontrolled inflammatory innate responses to virus in severe COVID-19 patients might lead to damage to targeted organs, both locally and systemically, which may be characterized by the unchecked influx of inflammatory cells into targeted sites and cytokine storm. However, uncertainty about the underlying immunopathogenesis, exact cascades of hypercytokinemia, as well as the timing of the fluctuations of some cytokines during the disease course require further investigation.

This study has some limitations. First, this is a relatively small cohort study, thus some results might not be representative of the severity characteristics of COVID-19. Second, due to hardly accessible to biopsy or autopsy of deceased cases, only 2 cases of pathological analysis were performed in this cohort, and the results might not be generalizable to all patients. Third, management of severe COVID-19 is rapidly evolving over time, and some treatment regimens for COVID-19 patients used in early- and middle- endemic periods of the SARS-CoV-2 outbreak were empirical.

In conclusion, this study addressed the characteristics and underlying immunopathology of severe COVID-19 through a comprehensive analysis of clinical and pathological features. Clinically, a panel of laboratory parameters, including the dynamic cytokines could be predictors of disease deterioration, and targeting cytokines' intervention such as Tocilizumab might be an alternative option for severe COVID-19 cases. Pathologically, the severe pulmonary damage was predominantly attributed to both SARS-CoV-2 caused cytopathy and immunopathologic damage. Therefore, strategies toward pulmonary recruitment and abnormal activation of mononuclear cells/macrophages and neutrophils through suppressing the inflammatory storm might improve the outcomes of severe COVID-19 patients.

MATERIALS AND METHODS

Patients

Sixty-nine confirmed COVID-19 patients included in the present study were consecutively admitted to designated centers in Beijing from Jan 20th 2020 to Mar 20th, 2020. All patients with COVID-19 enrolled in this study were diagnosed and classified by severity according to the Guidelines for the Diagnosis and Treatment of New Coronavirus Pneumonia (version 5) published by the National Health Commission of China. Laboratory confirmation of COVID-19 was performed at the Centers for Disease Control (CDC) with RT-PCR detection reagents. Severe patients met at least one of the following criteria: (1) shortness of breath with a RR ≥ 30 times/min, (2) oxygen saturation (resting state) ≤ 93%, or (3) PaO2 / FiO2 ≤ 300mmHg.

Data collection

Epidemiological, clinical, laboratory and radiological data were obtained from electronic medical records. The data were reviewed by a trained team of physicians. The date of the diagnosis of a severe case was determined as the day the patient first met the severity criteria according to medical records. The final date of follow-up was Mar 29th, 2020.

Radiology

Digital chest radiographs and computed tomography (CT) were performed at admission and during hospitalization. The images were assessed by using a picture archiving and communication system viewer. All chest radiographs and CT images were reviewed independently by three trained radiologists with ten years of experience. Final assessments were reached by consensus. Scoring was performed according to the following criteria of 7 stages: 0, bilateral lungs showing clear texture; 1, bilateral lungs showing mild shadows; 2, single small patch shadow; 3, unilateral lung showing multiple patch shadows; 4, bilateral lungs showing multiple patch shadows; 5, unilateral lung showing consolidation; 6, bilateral lungs showing consolidation (less than 50%) and 7, bilateral lungs showing consolidation (more than 50%).

Clinical specimen collection

Clinical specimens for COVID-19 diagnostic testing were obtained in accordance with China CDC guidelines. Throat-swabs and blood specimens were obtained and maintained in viral-transport medium. On the admission day, blood samples were collected before any medications. During hospitalization, all blood samples were collected during fasting time. Serum samples were collected in serum separator tubes and then centrifuged in accordance with China CDC guidelines. Postmortem lung tissues were biopsied from two patients who died of severe COVID-19 as described with informed consent.

Circulating cytokine and chemokine measurement

The concentrations of inflammatory cytokines including IL6 (#YZB/UK 4438-2014, SIEMENS, Gwynedd, UK), IL8 (#YZB/UK 4439-2014, SIEMENS, Gwynedd, UK), IL1β(#YZB/UK 4797-2014, SIEMENS, Gwynedd, UK) and TNFα(#YZB/UK 2641-2012, SIEMENS, Gwynedd, UK) in serum specimens from COVID-19 patients were measured by chemiluminescence immunoassay according to manufacturer`s instruction. Quantification of IP10 (#ab100579, abcam, Cambridge, MA, USA), MCP1 (#ab179886, abcam, Cambridge, MA, USA) and RANTES (# ab174446, abcam, Cambridge, MA, USA) were measured by enzyme linked

immunosorbent assay according to manufacturer`s instruction. Triplicate tests of each independent sample were conducted.

Histopathology

Postmortem lung tissues obtained from patients with COVID-19 were fixed in 10% neutral buffered formalin, paraffin-embedded, sectioned at 4μm, de-waxed and rehydrated by standard procedures. The slides were stained with hematoxylin and eosin (H&E). Masson trichrome staining was used to assess collagen fibers in lung tissues according to the standard method. The tissues were stained with trichrome stain kit (#HT15-1KT, Sigma-Aldrich, St. Louis., MO, USA), then with Biebrich scarlet-acid fuchsin, and differentiated in phosphomolybdic-phosphotungstic acid solution for 10–15 min. The sections were stained with aniline blue solution for 5 min, differentiated in glacial acetic solution for 5 min, dehydrated with 95% ethanol, cleared with xylene and mounted. The stained sections were observed with a light microscope.

Transmission electron microscope (TEM)

TEM was performed to observe the ultrastructural changes and SARS-CoV-2 viral particles in lung tissues. In detail, the specimens were fixed with 2.5% glutaraldehyde, postfixed with 1% osmium tetraoxide, rehydrated in a graded series of ethanol concentrations, and embedded in SPIPON812 resin. The ultrathin slides were sectioned with microtome (Leica EM UC6) at approximately 70 nm, collected on copper grids and stained with uranyl acetate and lead citrate. Images were obtained with TEM (JEM-1011 120 kv, Tokyo, Japan).

Immunohistochemistry

Immunohistochemical examination of tissue samples was performed based on a standard protocol. Paraffin-embedded tissue sections were deparaffinized and rehydrated in a graded series of ethanol concentrations. Antigen retrieval was performed by heating the sections at 96°C in 0.01 mol/L citrate buffer (pH 6.0) for 30 min. Sections were immersed in 3% hydrogen peroxide to eliminate endogenous peroxidase activity. Slides were then incubated with primary antibodies overnight at 4°C at optimal dilutions. Primary antibodies included anti-human CD4 (#ZM-0418, ORIGENE, Rockville, MD, USA,1:100), CD8 (#ZM-0508, ORIGENE, Rockville, MD, USA, 1:50), CD68 (#Kit-0026, Thermo Fisher Scientific, Waltham, MA, USA, 1:200), MPO (#ZA-0197, Sigma-Aldrich, St. Louis., MO, USA, 1:150), SPB (#ZM-0226, Zeta Corporation, Sierra Madre, CA, USA, 1:100), CK7(#Kit-0021, Thermo Fisher Scientific, Waltham, MA, USA, 1:100), and gasdermin D (#96458 Cell Signaling Technology, Danvers, MA, USA, 1:200).

Terminal deoxynucleotidyl transferase-mediated dUTP nick-end labelling (TUNEL)

To assess cell apoptosis, a TUNEL assay was performed on tissue slides according to manufacturer's instructions. The sections were deparaiffinized, rehydrated, and pre-treated with proteinase K (DNase free) (#ST532, Beyotime Biotechnology, Beijing, China). The sections were then washed with PBS, and stained with a mixture of TdT and dUTP at 37°C for 60 min (#C1086, Beyotime Biotechnology, Beijing, China). The stained apoptotic cells were observed with a fluorescence microscope.

RNAscope in situ hybridization

In situ hybridization assay was performed using the RNAscope® 2·5 HD-Brown assay (#322310, Advanced Cell Diagnostics,

Newark, CA, USA) to measure SARS-CoV-2 RNA in formalin-fixed paraffin-embedded (FFPE) tissue sections. RNAscope® Probe V-nCoV2019-S for SARS-CoV-2 (#848561, target region: 21631-23303 of NC_045512.2), RNAscope® Positive Control Probe-Hs-PPIB (#313901, target region: 139-989 of NM_000942.4), and RNAscope® Negative Control Probe-DapB (#310043, target region: 414-862 of EF191515) were performed on serial sections. The assay was performed according to the standard manufacturer's protocol. Probes were hybridized to a cascade of signal amplification molecules, culminating in the binding of HRP-labeled probes. The assay enhanced the signal further with additional amplification (AMP) steps. Hybridize amplification rounds 1-6 (AMP1-6) were performed. In AMP 1, each slide was taken at a time from the Tissue-Tek® Slide Rack and the excess liquid was removed from the slides. The slides in HybEZTM Humidity Control Tray were inserted into oven for 30 min at 40°C for AMP1 (15 min at 40°C for AMP2, 30 min at 40°C for AMP3, 15 min at 40°C for AMP4, 30 min at RT for AMP5, and 15 min at RT for AMP6). Excess liquid was quickly removed, and the slide was placed in a Tissue-Tek® Slide Rack submerged in the Tissue-Tek® Staining Dish filled with wash buffer. Slides were washed for 2 min at room temperature (RT) with occasional agitation. The slides were then stained with DAB substrate per section and the signals were detected. Slide counterstain was performed in hematoxylin staining solution for 2 min at RT. The hybridization sections were dehydrated in 70% ethyl alcohol, 95% ethyl alcohol and xylene, and mounted. The hybridization signals were captured using an Aperio AT2 digital slide scanner equipped with a 40x objective (Leica Biosystems Inc., Buffalo Grove, IL, USA).

Statistical analysis

Continuous variables were summarized as means ± standard deviations (SD) or medians (interquartile ranges, IQR) as appropriate, whereas categorical variables were presented as number (percentage). To compare the continuous variables between two groups, student t test or Mann-Whitney U test was performed, as appropriate. A generalized linear mixed model was used to compare repeated measures (non-normal distribution). The Chi-square test and Fisher’s exact test were used for comparing categorical variables. All statistical tests were two-sided, and a p value less than 0.05 was defined as statistically significant. Data were analyzed using SAS 9.4 (SAS Institute, Cary, NC, USA).

Study approval

Sample collection and analysis of cases were performed strictly in accordance with the regulations issued by the National Health Commission of China and the ethical standards formulated in the Helsinki Declaration. This study was approved by the Institutional Review Board of The Fifth Medical Center of PLA General Hospital, China.

Authors Contributions: JZ contributed to study concept and design, clinical and pathological analysis, study supervision and critical revision of the manuscript; JJ contributed to study supervision, clinical data collection and analysis; SLi, LJ, XL, YW contributed to analysis and interpretation of data, make tables and figures, literature search and writing of the manuscript; FL contributed to clinical data collection, analysis, interpretation and writing of the manuscript; BL contributed to laboratory specimen collection and measurement; TJ contributed to clinical data collection and analysis; WA contributed to radiology data collection and analysis; SL contributed to immunohistochemistry staining and pathological analysis; HL contributed to statistical analysis; PX and LZhang contributed to pathological experiments; LZ contributed to making figures; HW, JK, JL contributed to electron microscope examination and analysis; YL contributed to clinical data collection; JM, LH, CZ and SZ contributed to clinical data and pathological specimen collection and analysis. SLi, LJ, XL, FL, YW, BL and TJ contributed equally to this article. The order in which they are listed was determined by workload.

Acknowledgments

We thank all the patients and their families involved in this study, as well as numerous doctors, nurses and civilians working together to fight against the COVID-19.

REFERENCES

1. Phelan AL, Katz R, and Gostin LO. The Novel Coronavirus Originating in Wuhan, China: Challenges for Global Health Governance. *JAMA.* 2020.
2. Wang D, Hu B, Hu C, Zhu F, Liu X, Zhang J, et al. Clinical Characteristics of 138 Hospitalized Patients With 2019 Novel Coronavirus-Infected Pneumonia in Wuhan, China. *JAMA.* 2020.
3. Chen N, Zhou M, Dong X, Qu J, Gong F, Han Y, et al. Epidemiological and clinical characteristics of 99 cases of 2019 novel coronavirus pneumonia in Wuhan, China: a descriptive study. *Lancet.* 2020;395(10223):507-13.
4. Ai T, Yang Z, Hou H, Zhan C, Chen C, Lv W, et al. Correlation of Chest CT and RT-PCR Testing in Coronavirus Disease 2019 (COVID-19) in China: A Report of 1014 Cases. *Radiology.* 2020:200642.
5. Huang C, Wang Y, Li X, Ren L, Zhao J, Hu Y, et al. Clinical features of patients infected with 2019 novel coronavirus in Wuhan, China. *Lancet.* 2020;395(10223):497-506.
6. Chen G, Wu D, Guo W, Cao Y, Huang D, Wang H, et al. Clinical and immunological features of severe and moderate coronavirus disease 2019. *J Clin Invest.* 2020.
7. C H, Y W, X L, L R, J Z, Y H, et al. Clinical features of patients infected with 2019 novel coronavirus in Wuhan, China. *Lancet (London, England).* 2020.
8. Xu Z, Shi L, Wang Y, Zhang J, Huang L, Zhang C, et al. Pathological findings of COVID-19 associated with acute respiratory distress syndrome. *Lancet Respir Med.* 2020.
9. Qin C, Zhou L, Hu Z, Zhang S, Yang S, Tao Y, et al. Dysregulation of immune response in patients with COVID-19 in Wuhan, China. *Clin Infect Dis.* 2020.
10. Li JY, You Z, Wang Q, Zhou ZJ, Qiu Y, Luo R, et al. The epidemic of 2019-novel-coronavirus (2019-nCoV) pneumonia and insights for emerging infectious diseases in the future. *Microbes Infect.* 2020.
11. Wong CK, Lam CW, Wu AK, Ip WK, Lee NL, Chan IH, et al. Plasma inflammatory cytokines and chemokines in severe acute respiratory syndrome. *Clin Exp Immunol.* 2004;136(1):95-103.
12. Wang WK, Chen SY, Liu IJ, Kao CL, Chen HL, Chiang BL, et al. Temporal relationship of viral load, ribavirin, interleukin (IL)-6, IL-8, and clinical progression in patients with severe acute respiratory syndrome. *Clin Infect Dis.* 2004;39(7):1071-5.
13. Zhang Y, Li J, Zhan Y, Wu L, Yu X, Zhang W, et al. Analysis of serum cytokines in patients with severe acute respiratory syndrome. *Infect Immun.* 2004;72(8):4410-5.
14. Chen G, Wu D, Guo W, Cao Y, Huang D, Wang H, et al. Clinical and immunologic features in severe and moderate Coronavirus Disease 2019. *J Clin Invest.* 2020.
15. R C, AR F, R V, M M, J Z, DK M, et al. Dysregulated Type I Interferon and Inflammatory Monocyte-Macrophage Responses Cause Lethal Pneumonia in SARS-CoV-Infected Mice. *Cell host & microbe.* 2016;19(2):181-93.
16. Chen L, Xiong J, Bao L, and Shi Y. Convalescent plasma as a potential therapy for COVID-19. *Lancet Infect Dis.* 2020;20(4):398-400.
17. Grein J, Ohmagari N, Shin D, Diaz G, Asperges E, Castagna A, et al. Compassionate Use of Remdesivir for Patients with Severe Covid-19. *N Engl J Med.* 2020.

18. Cao B, Wang Y, Wen D, Liu W, Wang J, Fan G, et al. A Trial of Lopinavir-Ritonavir in Adults Hospitalized with Severe Covid-19. *N Engl J Med.* 2020.

19. Costanzo M, De Giglio MAR, and Roviello GN. SARS CoV-2: Recent Reports on Antiviral Therapies Based on Lopinavir/Ritonavir, Darunavir/Umifenovir, Hydroxychloroquine, Remdesivir, Favipiravir and Other Drugs for the Treatment of the New Coronavirus. *Curr Med Chem.* 2020.

20. Tu YF, Chien CS, Yarmishyn AA, Lin YY, Luo YH, Lin YT, et al. A Review of SARS-CoV-2 and the Ongoing Clinical Trials. *Int J Mol Sci.* 2020;21(7).

21. Russell CD, Millar JE, and Baillie JK. Clinical evidence does not support corticosteroid treatment for 2019-nCoV lung injury. *Lancet.* 2020;395(10223):473-5.

22. Feldmann M, Maini RN, Woody JN, Holgate ST, Winter G, Rowland M, et al. Trials of anti-tumour necrosis factor therapy for COVID-19 are urgently needed. *Lancet.* 2020.

23. DR G. The Coming Decade of Cell Death Research: Five Riddles. *Cell.* 2019;177(5):1094-107.

24. SM M, R K, and TD K. Molecular mechanisms and functions of pyroptosis, inflammatory caspases and inflammasomes in infectious diseases. *Immunological reviews.* 2017;277(1):61-75.

25. Bergsbaken T, Fink SL, den Hartigh AB, Loomis WP, and Cookson BT. Coordinated host responses during pyroptosis: caspase-1-dependent lysosome exocytosis and inflammatory cytokine maturation. *J Immunol.* 2011;187(5):2748-54.

26. Shi J, Gao W, and Shao F. Pyroptosis: Gasdermin-Mediated Programmed Necrotic Cell Death. *Trends Biochem Sci.* 2017;42(4):245-54.

27. Zhang Z, Zhang Y, Xia S, Kong Q, Li S, Liu X, et al. Gasdermin E suppresses tumour growth by activating anti-tumour immunity. *Nature.* 2020;579(7799):415-20.

28. Dean GA, Olivry T, Stanton C, and Pedersen NC. In vivo cytokine response to experimental feline infectious peritonitis virus infection. *Vet Microbiol.* 2003;97(1-2):1-12.

Figure 1.

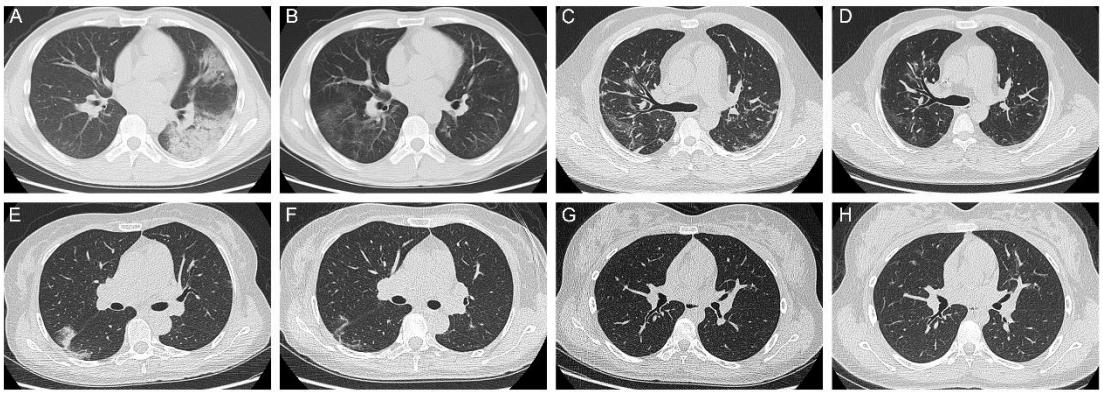

Figure 1. CT images of 2 severe patients and 2 non-severe COVID-19 patients. (A) CT image of a 33-year-old man showing bilateral ground-glass opacities (GGO) partially fused into consolidation at onset of hospitalization and (B) mild GGO in the bilateral lungs. (C) CT image of a 51-year-old man showing bilateral ground-glass opacities at onset of hospitalization and (D) multiple slightly high dense shadows in the bilateral lungs. (E) CT image of a 53-year-old female showing bilateral ground-glass opacities at the onset of hospitalization and (F) absorption after recovery. (G) CT image of a 17-year-old woman showing mild consolidation at the onset of hospitalization and (H) absorption after recovery.

Figure 2.

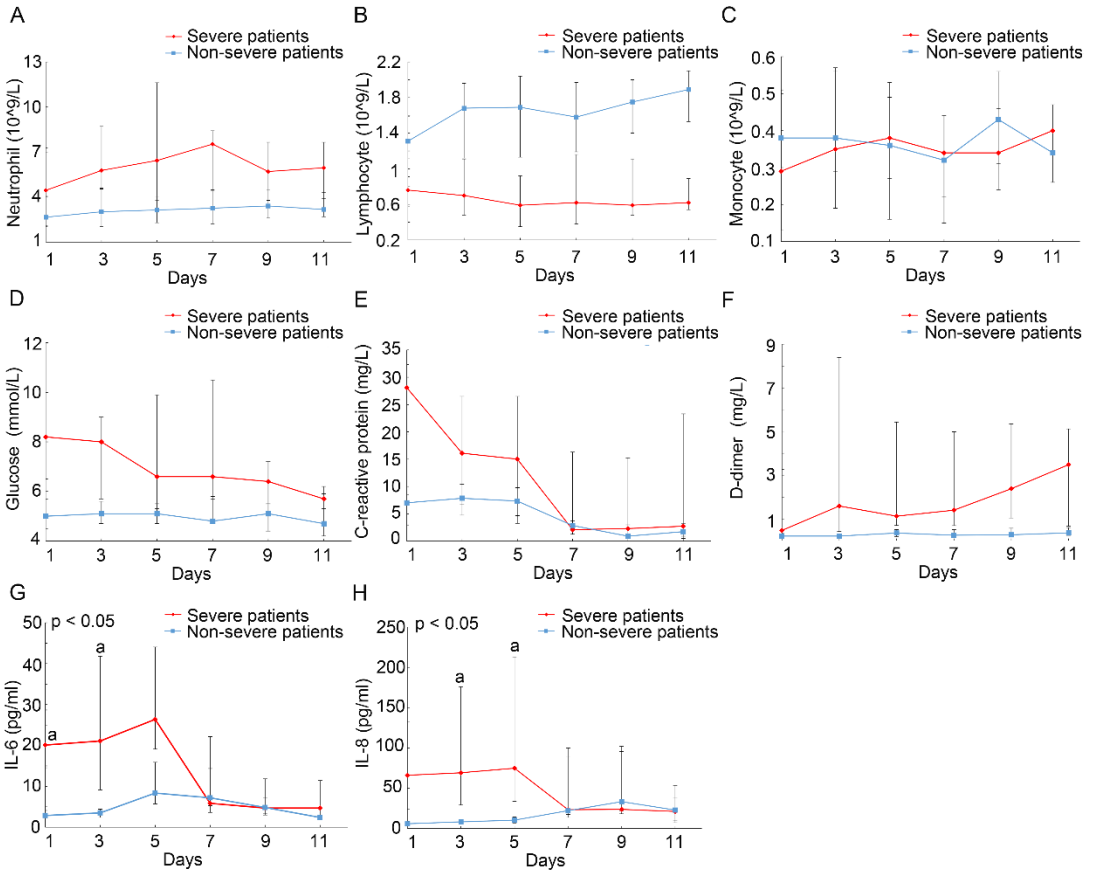

Figure 2. Dynamics of blood (A) neutrophils, (B) lymphocytes, (C) monocytes, (D) glucose, (E) C-reactive protein, (F) D-dimer, (G) IL6 and (H) IL8 between severe patients (n=21) and non-severe patients (n=25). Data represent as median±IQR. A generalized linear mixed model was used to compare repeated measures (non-normal distribution). Data were presented as the mean of triplicate measurements.

Figure 3.

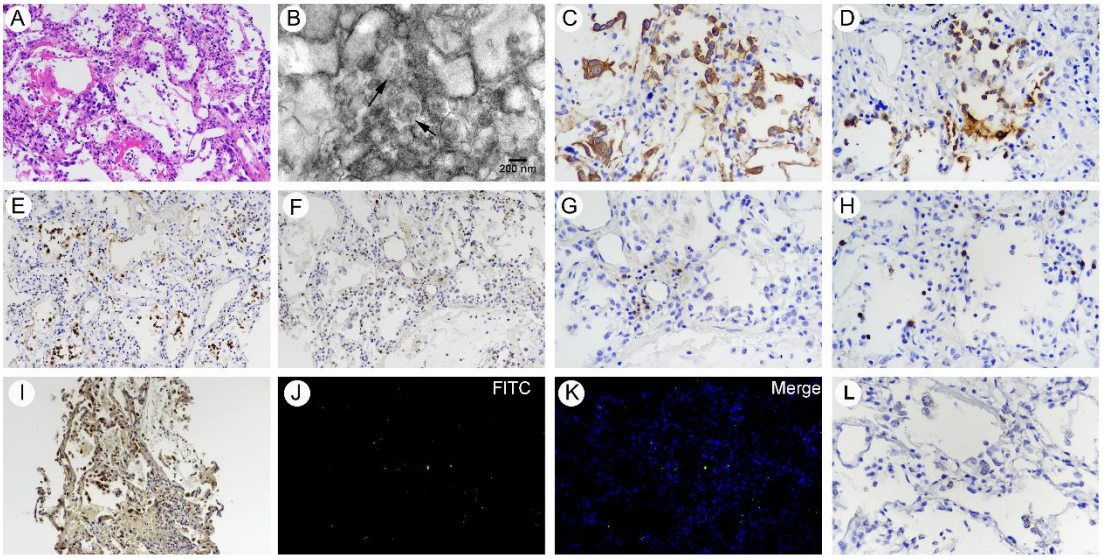

Figure 3. Postmortem lung biopsy specimens from case 1. (A) Lung tissue showing pulmonary edema with hyaline membranesand desquamation of alveolar epithelial cells (H&E staining, original magnification ×200). (B) Ultrastructural image showing cytoplasmic viral particles in a type II pneumocyte (arrow) with swollen mitochondria and dilated endoplasmic reticulum (original magnification ×20000). (C) CK7 positive cells reflecting pneumocytes (original magnification ×200). (D) SPB-positive cells indicating type II pneumocytes with marked vacuolation and mild hyperplasia (original magnification ×200). (E) Increased CD68+ macrophages with cytomegaly mainly in alveolar spaces (original magnification ×200). (F) Immunohistochemical staining for MPO indicating a large number of interstitial infiltrated polymorphonuclear cells (original magnification ×200). (G) CD4+ and (H) CD8+ T cells distributed in the alveolar septal walls and interstitial areas (original magnification ×200). (I) Gasdermin D positivity indicating cell pyroptosis (original magnification ×200). (J-K) TUNEL staining showing apoptotic cells (original magnification ×200). (L) RNAscope in situ hybridization indicating SARS-CoV-2 nucleic acids which manifest as spotted brown particles (original magnification ×200).

Figure 4.

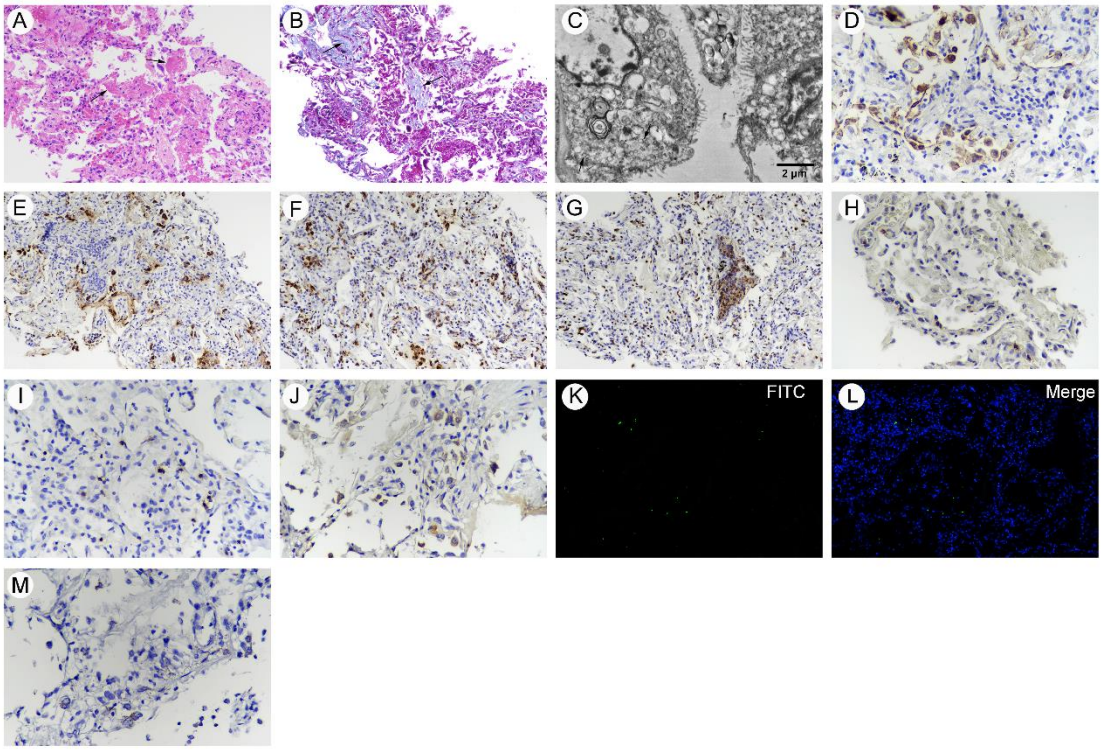

Figure 4. Postmortem lung biopsy from case 2. (A) H&E and (B) Masson's trichrome staining showing features of early interstitial and alveolar fibrosis, and mild pneumocyte hyperplasia, with focal exudative edema and hyaline membranes (arrow) in alveolar spaces. (C) Ultrastructural image showing cytoplasmic viral particles (arrow) characterized by spherical and spike-like projections in type II pneumocytes, with depleted laminar bodies, swollen mitochondria and dilated endoplasmic reticulum. (D) CK7 positive cells showing pneumocytes (original magnification ×200). (E) SPB-positive cells reflecting type II pneumocytes (original magnification ×200). (F) Abundantly increased CD68+ macrophages in alveolar spaces. (G) Immunohistochemical staining of MPO indicating numerous polymorphonuclear cells, aggregated in focal areas of bronchiolitis (original magnification ×200). (H) A few CD4+ and (I) CD8+ T cells were distributed in the alveolar septal walls and interstitial areas (original magnification ×200). (J) Gasdermin D positive cells representing cell pyroptosis (original magnification ×200). (K-L) TUNEL staining showing apoptotic cells (original magnification ×200). (M) RNAscope in situ hybridization indicating SARS-CoV-2 nucleic acids which manifest as spotted brown particles (original magnification ×200).

Table 1 Characteristics, treatment and outcomes of patients with COVID-19*

Characteristics	Severe patients N = 26	Non-severe patients N = 43	*P*
Age (year)	58 (45-75)	39 (29-53)	< 0.001
Sex			
Male	14 (53.8)	26 (60.5)	0.589
Female	12 (46.2)	17 (39.5)	
Exposure			
Hubei province exposure	13 (50.0)	23 (53.5)	0.779
Close contact with exposures	12 (46.2)	23 (53.5)	0.555
Both above	2 (7.7)	8 (18.6)	0.371
No exposure	3 (11.5)	5 (11.6)	1.000
Coexisting medical conditions			
Diabetes	5 (19)	3 (7)	0.143
Hypertension	9 (34.6)	8 (18.6)	0.135
Coronary disease	3 (11.5)	1 (2.3)	0.147
Chronic liver disease	3 (11.5)	0 (-)	0.050
Chronic respiratory system disease	4 (15)	3 (7)	0.413
Malignancy	1 (4)	0 (-)	0.377
Signs and symptoms			
Fever	25 (96.2)	34 (79.1)	0.110
Cough	20 (76.9)	20 (46.5)	0.013
Myalgia or fatigue	14 (53.9)	12 (27.9)	0.031
Dyspnea	7 (26.9)	1 (2.3)	0.004
Headache	5 (19.2)	10 (23.3)	0.695
Diarrhoea	3 (11.5)	6 (14.0)	1.000
Sore throat	5 (19.2)	12 (27.9)	0.418
More than one sign or symptom	25 (96.2)	28 (65.1)	0.003
Radiography			
0-3	1 (3.9)	18 (41.9)	< 0.001
4-7	25 (96.1)	25(58.1)	
Medications			
Interferon α2b	23 (88.5)	37 (86.1)	1.000
Lopinavir / Ritonavir	21 (80.8)	34 (79.1)	0.865
Corticosteroid	25 (96.2)	5 (11.6)	< 0.001

Intravenous immunoglobulin therapy	21 (80.8)	7 (16.3)	< 0.001
Intravenous antibiotics	23 (88.5)	7 (16.3)	< 0.001
Antifungal medication	12 (46.2)	0 (-)	< 0.001
ECMO	1 (3.9)	0 (-)	0.377
CRRT	4 (15.4)	0 (-)	0.017
Outcomes			
Recovery	22 (84.6)	38 (88.4)	0.221
Death	2 (7.7)	0 (-)	
Hospitalization	2 (7.7)	5 (11.6)	
Length of stay (day)	23 (17-28)	14 (7-19)	< 0.001

* Normally distributed continuous variables were expressed in mean ± standard deviation (SD), whereas other continuous variables were expressed in median (interquartile range [IQR]). Categorical variables were presented as counts (percentage). Qualitative and quantitative differences between 2 groups were analyzed by Chi-square test or Fisher exact test for categorical parameters and Student t test or Mann-Whitney U test for continuous parameters as appropriate.

Abbreviations: ECMO, extracorporeal membrane oxygenation; CRRT, continuous renal replacement therapy.

Table 2 Laboratory findings of patients infected with COVID-19*

Characteristics	Severe patients N = 26	Non-severe patients N = 43	*P*
ABG			
PaO2/FiO2 > 300 (mmHg)#	262 (194-289)	393 (352-448)	< 0.001
> 300	3 (12)	22 (100)	
200-300	15 (60)	0 (-)	< 0.001
100-200	5 (20)	0 (-)	
≤ 100	2 (8)	0 (-)	
PaO_2 80-100 (mmHg)	68 (62-85)	85 (78-94)	0.001
SPO2 ≤ 93%‡	25 (96)	0 (-)	< 0.001
Respiratory rate≥ 30, per min‡	9 (35)	0 (-)	< 0.001
A-aDO_2 < 15 (mmHg)	52 (41-85)	23 (19-29)	< 0.001
Biochemistry			
Albumin 35-55 (g/L)	34 (31-38)	42 (38-44)	< 0.001
ALT 5-40 (U/L)	32 (15-69)	21 (14-36)	0.139
AST 5-40 (U/L)	27 (22-50)	24 (19-30)	0.251
GGT 11-50 (U/L)	50 (20-76)	22 (13-40)	< 0.001
LDH 109-245 (U/L)	247 (209-349)	197 (162-228)	< 0.001
Glucose 3.9-6.1 (mmol/L)	8.1 (5.7-10.0)	5.0 (4.8-5.7)	< 0.001
Blood routine			
WBC 3.97-9.15 (10^9/L)	6.40 (3.42-10.36)	4.75 (4.04-5.95)	0.083
NEUT 2-7 (10^9/L)	4.65 (2.11-8.79)	2.83 (1.98-3.51)	0.003
LYMPH 0.8-4.0 (10^9/L)	0.81 (0.50-1.11)	1.53 (1.28-2.02)	< 0.001
MONO 0.12-1.0 (10^9/L)	0.32 (0.14-0.42)	0.39 (0.30-0.50)	0.035
EO 0.02-0.5 (10^9/L)	0.00 (0.00-0.01)	0.04 (0.01-0.11)	< 0.001
BASO 0-1 (10^9/L)	0.01 (0.01-0.02)	0.01 (0.01-0.03)	0.160
Lymphocyte classification			
T LYMPH 690-2540 (/μl)	378 (258-576)	991 (740-1154)	< 0.001
CD4 LYMPH 410-1590 (/μl)	199 (128-325)	544 (364-667)	< 0.001
CD8 LYMPH 190-1140 (/μl)	134 (91-237)	417 (309-539)	< 0.001
B LYMPH 90-660 (/μl)	92 (56-135)	163 (126-224)	< 0.001
NK LYMPH 90-590 (/μl)	122 (51-162)	186 (122-302)	0.005
CD4/CD8 0.68-2.47	1.40 (0.79-2.08)	1.18 (0.96-1.58)	0.611

Coagulation profile			
Fibrinogen 2.0-4.0 (g/L)	4.13 (3.03-4.82)	2.78 (2.15-3.25)	0.002
D-dimer < 0.55 (mg/L)	0.56 (0.36-3.26)	0.23 (0.17-0.31)	< 0.001
Cytokine			
IL8 (pg/ml)	13.1 (11.4-15.9)	7.8 (6.4-10.4)	< 0.001
IL1β (pg/ml)	9.9 (6.0-18.3)	7.5 (6.8-8.7)	0.215
TNFα (pg/ml)	7.4 (6.7-8.7)	5.0 (4.8-6.08)	< 0.001
RANTES (pg/ml)	2272 (2236-2308)	2074 (1997-2170)	< 0.001
MCP1 (pg/ml)	264 (205-390)	134 (104-181)	0.001
IP10 (pg/ml)	863 (460-1249)	372 (281-558)	< 0.001
IL6 (pg/ml)	24.6 (17.9-45.0)	8.4 (5.7-15.9)	< 0.001
Infection			
CRP 0.068-8.2 (mg/L)	22.2 (6.8-37.5)	4.2 (1.6-8.2)	< 0.001
Procalcitonin 0-0.5 (ng/ml)	0.06 (0.04-0.09)	0.05 (0.04-0.06)	0.114
ESR 0-15 (mm/60min)	54 (36-70)	13 (7-20)	< 0.001
Ferritin 30-400 (ng/ml)	645 (440-1422)	254 (81-397)	< 0.001

* Normally distributed continuous variables were expressed in mean ± standard deviation (SD), whereas other continuous variables were expressed in median (interquartile range [IQR]). Categorical variables were presented as counts (percentage). Qualitative and quantitative differences between 2 groups were analyzed by Chi-square test or Fisher exact test for categorical parameters and Student t test or Mann-Whitney U test for continuous parameters as appropriate.

Data of PaO2/FiO2 were available in 25 severe patients and 22 non-severe patients, respectively.

‡ Data of SPO2 were available in 42 non-severe patients.

Abbreviations: ABG, arterial blood gas; PaO2, partial pressure of oxygen; FiO2, fraction of inspiration oxygen; SPO2, surplus pulse oxygen; A-aDO2, alveolar-arterial oxygen partial pressure difference; ALT, alanine aminotransferase; AST, aspartate aminotransferase; GGT, γ-glutamyl transferase; LDH, lactate dehydrogenase; WBC, white blood cell; NEUT, absolute neutrophil count; LYMPH, absolute lymphocyte value; MONO, absolute monocyte count; EO, absolute eosinophil count; BASO, absolute basophilic count; NK, natural killer cell; CRP, C-reactive protein; ESR, erythrocyte sedimentation rate.